ChemComm

COMMUNICATION

View Article Online
View Journal | View Issue

Confinement stabilises single crystal vaterite rods†

Anna S. Schenk, Eduardo J. Albarracin, Yi-Yeoun Kim, Johannes Ihli and Fiona C. Meldrum*

Cite this: *Chem. Commun.*, 2014, 50, 4729

Received 11th February 2014,
Accepted 24th March 2014

DOI: 10.1039/c4cc01093k

www.rsc.org/chemcomm

Single-crystals of vaterite, the least-stable anhydrous polymorph of $CaCO_3$, are rare in biogenic and synthetic systems. We here describe the synthesis of high aspect ratio single crystal vaterite rods under additive-free conditions by precipitating $CaCO_3$ within the cylindrical pores of track-etch membranes.

The widely studied mineral system $CaCO_3$ is rather unusual amongst inorganic compounds in that it has three crystalline polymorphs (of composition $CaCO_3$) – calcite, aragonite and vaterite – all of which can be accessed under ambient, aqueous conditions.[1] As a result, $CaCO_3$ is widely used as a model system for studying polymorph selection. Calcite is the most stable polymorph under ambient conditions and aragonite only slightly less stable; both are common biominerals. Vaterite is the thermodynamically least stable modification of anhydrous $CaCO_3$. While it does not appear geologically and is rare as a biomineral, there are some exceptions,[2,3] such as the micrometer-sized spicules of the ascidian *Herdmania momus*. The structure of this biomineral has recently been studied in detail, showing that the spicules are relatively defect-free single crystals of vaterite.[4]

The mechanism by which biology generates such large single crystals of vaterite is intriguing. Synthetically, vaterite is often observed as a transient phase that converts to calcite *via* dissolution–reprecipitation.[5] The rate is determined by the reaction conditions and the presence of organic additives.[6] It is very difficult to precipitate pure vaterite in the absence of additives, as highlighted by the recent use of a droplet-based microfluidic system to generate pure vaterite particles.[7] Vaterite also primarily forms as spherulitic polycrystalline aggregates,[8] such that single crystal vaterite is particularly rare. The only exceptions we have identified are high temperature syntheses,[9–11] and room temperature syntheses in the presence of soluble organic additives,[12] ammonium ions[13] and under octadecylamine monolayers.[14] Porous hexagonal prisms of vaterite have been produced in a gelatine matrix under hydrothermal conditions,[15] and single crystal vaterite tubes through water-electrolysis.[16]

In this article, we explore the possibility that organisms use the confinement intrinsic to biomineralisation processes to generate single crystals of vaterite. Highlighting the role of microenvironment in controlling polymorphism, all three $CaCO_3$ polymorphs were selectively precipitated within uniaxially deformed gelatine films in the presence of poly(aspartic acid) according to the degree of deformation of the film and the concentration of soluble additive.[17] Similarly, a substrate constructed from β-chitin, silk fibroin and soluble macromolecules was formed as a mimic of the organisation present in molluscs, and calcite or aragonite could be precipitated within the chitin when the macromolecules were extracted from calcitic or aragonitic shell layers respectively.[18] It is stressed, however, that both of these examples combine both additives and structured environments to gain control over crystal nucleation and growth. More recently, studies have shown that amorphous calcium carbonate (ACC) can be stabilised with respect to calcite in the absence of additives in small volumes.[19–21]

To investigate the possibility of using confinement alone to control $CaCO_3$ polymorph, $CaCO_3$ was precipitated within the pores of track-etched (TE) membranes in the absence of additives. This system has previously been used to generate single crystal calcite rods at low temperature[22,23] or by the addition of poly(acrylic acid) (PAA).[24] The membranes were placed in a $CaCl_2$ solution and were exposed to ammonium carbonate vapour (Fig. 1).[25] Two membrane types with 200 nm pores were employed, as purchased from Millipore and Sterlitech. Both were manufactured from polycarbonate and possessed a coating of polyvinyl pyrrolidone (PVP), a linear, non-ionic, water-soluble polylactam which increases hydrophilicity and improves filtration performance in aqueous media.

Precipitation of $CaCO_3$ within the Millipore membranes ($[Ca^{2+}]$ = 10 mM) led to the formation of a high yield of intra-membrane particles, where these formed in ~80% of the available pores (Fig. 2a and b; Fig. S1, ESI†). These particles exhibited rod-like morphologies and aspect ratios of ≈50, demonstrating that

School of Chemistry, University of Leeds, Leeds, LS2 9JT, UK.
E-mail: f.meldrum@leeds.ac.uk

† Electronic supplementary information (ESI) available: Full description of experimental methods, and supplementary data and figures. See DOI: 10.1039/c4cc01093k

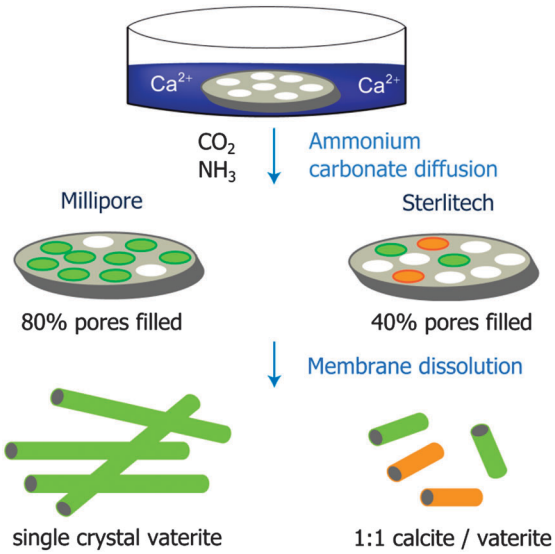

Fig. 1 Schematic diagram showing $CaCO_3$ precipitation within track-etch membranes. Membranes purchased from Millipore and Sterlitech were employed, and high aspect ratio, single crystal rods of vaterite were obtained in the Millipore membranes, while shorter calcite or vaterite particles were isolated from the Sterlitech templates.

they filled the entire 10 μm long pore. Transmission electron microscopy (TEM) showed that they were uniform in structure (Fig. 2c), even though the surfaces often appeared rough (Fig. 2b). Structural investigation of these rods using selected area electron diffraction (SAED) revealed that the vast majority were single crystals of vaterite (Fig. 2c, inset) and only a minor sub-population (~5%) of calcite rods was identified. The single crystal character of the nanorods was further demonstrated using high resolution TEM which showed well-resolved, continuous lattice fringes over wide areas (Fig. 2d), while Raman microscopy of bundles of rods also confirmed that vaterite was the major polymorph (Fig. S2, ESI†). Finally, the crystals precipitated on the surfaces of the membranes were characterised. These provide an effective control as they grow in association with the membrane but in bulk solution rather than in confinement. Light microscopy, scanning electron microscopy (SEM) and Raman microscopy showed that these surface crystals were calcite rhombohedra, together with ~5% vaterite particles (Fig. S3, ESI†).

The Sterlitech membranes, in contrast, yielded very little intra-membrane material under the same reaction conditions, where this comprised a roughly 1:1 mixture of vaterite and calcite. The few nanorods produced were ≈2–5 μm in length, demonstrating incomplete mineral infiltration (Fig. 2e). Again, calcite rhombohedra formed on the membrane surfaces, in similar amounts to that seen on the Millipore membranes. To compare with our previous work, substantial filling of the Sterlitech membrane pores could only be achieved when PAA was added to the reactant solution, where this polyelectrolyte promotes the formation of a liquid-like precursor to $CaCO_3$[26,27] that drives infiltration by capillary action.[24] However, with PAA present, calcite was the dominant polymorph in both membranes.[24]

As polymorph production in the $CaCO_3$ system is strongly dependent on the solution supersaturation,[8,28] the influence of

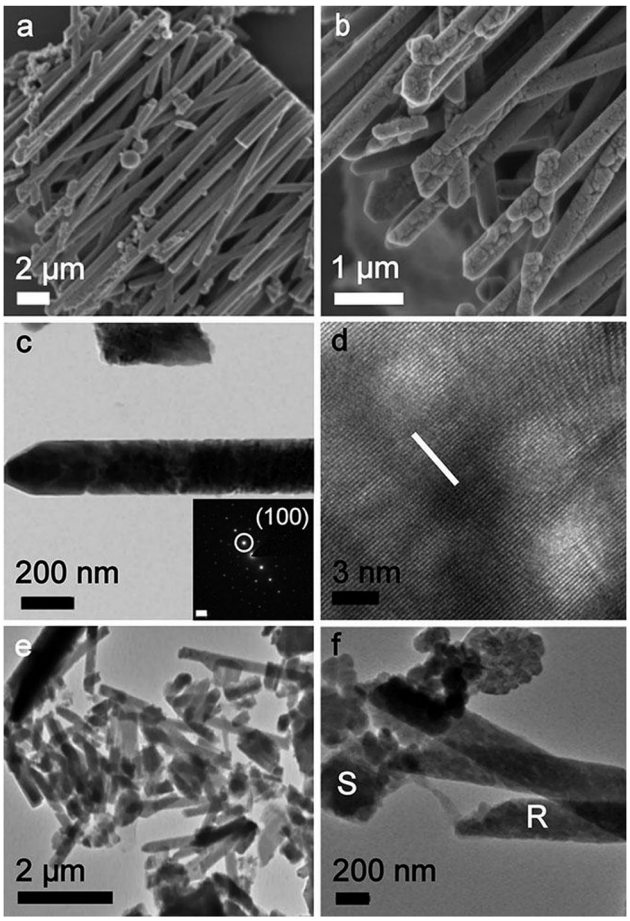

Fig. 2 $CaCO_3$ crystals precipitated within the pores of Millipore (a–d) and Sterlitech (e and f) membranes. (a, b) SEM images of rods produced at $[Ca^{2+}]$ = 10 mM. (c) A TEM image and corresponding electron diffraction pattern of a single crystal vaterite nanorod (scale bar inset = 2 nm^{-1}). (d) HRTEM image of a vaterite nanorod showing the continuity of the crystal lattice. The white bar corresponds to the normal to the {100} planes. (e) TEM image of particles precipitated in Sterlitech membranes at $[Ca^{2+}]$ = 10 mM. (f) TEM image of high aspect ratio vaterite rods (R) generated at $[Ca^{2+}]$ = 100 mM. Under these reaction conditions the crystals formed on the surface of the membranes (S) are also vaterite.

the reaction conditions on intra-membrane precipitation was also studied. While little intra-pore precipitation occurred for either membrane at $[Ca^{2+}]$ = 0.5 mM, $[Ca^{2+}]$ = 100 mM gave good infiltration and long rods in both types of membranes (Fig. 2f). Further, all mineral precipitated under these conditions – either within the pores or on the membrane surfaces – was vaterite. Analysis of the rods using SAED showed that those in the Sterlitech membranes were principally polycrystalline, although some domains diffracted as single crystals (Fig. S4, ESI†). As an effect of the faster growth kinetics, the single-crystallinity of the rods in the Millipore membranes was also disrupted, and polycrystalline domains comprised ≈20% of the rods (Fig. S5, ESI†).

That unmodified rhombohedral calcite crystals precipitated on the surfaces of both membranes at $[Ca^{2+}]$ = 10 mM provided very strong evidence that vaterite formation within the Millipore membranes was not the result of soluble additives released from the membrane. Confirming this important analysis, membranes soaked

in water for three days prior to use gave identical results to those achieved with unsoaked membranes, and $CaCO_3$ precipitated with high concentrations of PVP ([PVP] = 1 g L^{-1}, [Ca^{2+}] = 10 mM) resulted in rhombohedral calcite crystals and very little vaterite (Fig. S6, ESI†). Finally, $CaCO_3$ infiltration of the Sterlitech membranes in the presence of PVP ([PVP] = 0.5 or 1 g L^{-1}) gave no increase in the yield or length of the $CaCO_3$ rods.

The differences in $CaCO_3$ precipitation within the Sterlitech and Millipore membranes must originate from variations in the environments offered by the different membrane pores. Both types of membranes, which showed similar pore size distributions by SEM (Fig. S7, ESI†), were therefore characterised with respect to their surface chemistry and topography using methods including IR spectroscopy, X-ray photoelectron spectroscopy, BET and AFM. These analyses, which are detailed in the Supporting Information (Fig. S8–S10, ESI†), revealed only minor differences in the surface roughness and no compositional variations.

Considering then the mechanism of polymorph control active within the membrane pores, it is clear that very subtle differences in the microenvironments within the pores must drive the observed effects on $CaCO_3$ precipitation. These may comprise differences in the density or conformation of the chemical species lining the membrane pores where this is consistent with observations that conformation changes in self-assembled monolayers (SAMs) can dramatically affect the vaterite/calcite ratio.[29] We also speculate that the Millipore membranes, which additionally show superior infiltration characteristics, may exhibit an organisation of the surface coating which leads to an accumulation of Ca^{2+} ions within the pores. This would result in a higher local supersaturation, which is associated with the stabilisation of vaterite.[28] Indeed, charge accumulation has previously been identified as a dominating factor controlling the polymorphism in template-directed growth of $CaCO_3$.[14,30]

That the vaterite forms as single crystals within the membrane pores while it so readily precipitates as polycrystalline aggregates in bulk solution is also intriguing and demonstrates that the membrane pores must provide environments which limit vaterite nucleation. Once formed, a nucleus can then grow with limited competition to give a single crystal product. It is noted that although ACC is the first phase to precipitate at the concentrations employed here (Fig. S11, ESI†), it is very short-lived as compared with the timescale of membrane infiltration, where complete filling of the pores is observed after $\approx$2 hours. This strongly suggests that $CaCO_3$ deposition within the membranes relies on the diffusion of ions into the pores rather than an uptake of ACC as occurs in the presence of the polyelectrolytes such as PAA. Finally, the considerable stability of the vaterite single crystals ($\geq$4 days) within membranes immersed in the reaction solution is also attributed to their confinement. As the recrystallisation of vaterite to calcite can only proceed *via* dissolution–reprecipitation at room temperature,[31] the confines of the pores retard recrystallisation by reducing the contact of the vaterite particles with solution to the exposed ends of the rods.

Despite having been the subject of intense study over the last 40–50 years, understanding of how organisms control $CaCO_3$ polymorphism has remained elusive, with effort focussing on the extraction and characterization of soluble additives from within calcite and aragonite biominerals. While we cannot of course provide a conclusive explanation for the selectivity over polymorph and structure observed here, our results provide an intriguing demonstration that subtle changes in microenvironment can have significant effects on polymorph production. Selectivity of vaterite over calcite was achieved, where this is likely to derive from the contrasting nucleation environments provided within the pores. Just as striking is the production of single crystals of vaterite in the absence of additives at room temperature. Again, this must be determined at nucleation through the production of a single nucleus, or a small number of nuclei that then grow competitively. Going beyond confinement effects alone, it is then interesting to note that these processes can be further modified by the addition of soluble additives to the system such that the single crystals of vaterite are replaced by single crystals of calcite through addition of poly(acrylic acid) to the reaction solution. These results are clearly of great relevance to any situation in which crystallisation occurs in confinement, and future work will investigate the role of surface chemistry further by tailoring the functionalisation of the membrane pores.

This work was supported by an EPSRC Programme Grant (AS and FCM, EP/I001514/1) which funds the Materials in Biology (MIB) consortium and an EPSRC Leadership Fellowship (FCM, YYK and JI, EP/H005374/1).

Notes and references

1 F. C. Meldrum, *Int. Mater. Rev.*, 2003, **48**, 187–224.
2 A. M. Oliveira, M. Farina, I. P. Ludka and B. Kachar, *Naturwissenschaften*, 1996, **83**, 133–135.
3 L. Qiao, Q.-L. Feng and Z. Li, *Cryst. Growth Des.*, 2007, **7**, 275–279.
4 L. Kabalah-Amitai, B. Mayzel, Y. Kauffmann, A. N. Fitch, L. Bloch, P. U. P. A. Gilbert and B. Pokroy, *Science*, 2013, **340**, 454–457.
5 J. D. Rodriguez-Blanco, S. Shaw and L. G. Benning, *Nanoscale*, 2011, **3**, 265–271.
6 H. Wei, Q. Shen, Y. Zhao, D. J. Wang and D. F. Xu, *J. Cryst. Growth*, 2003, **250**, 516–524.
7 A. Yashina, F. Meldrum and A. deMello, *Biomicrofluidics*, 2012, **6**, 022001.
8 J. P. Andreassen, *J. Cryst. Growth*, 2005, **274**, 256–264.
9 R. Beck, E. Flaten and J.-P. Andreassen, *Chem. Eng. Technol.*, 2011, **34**, 631–638.
10 L. Dupont, F. Portemer and M. Figlarz, *J. Mater. Chem.*, 1997, **7**, 797–800.
11 S. R. Kamhi, *Acta Crystallogr.*, 1963, **16**, 770–772.
12 A.-W. Xu, M. Antonietti, H. Cölfen and Y.-P. Fang, *Adv. Funct. Mater.*, 2006, **16**, 903–908.
13 E. M. Pouget, P. H. H. Bomans, A. Dey, P. M. Frederik, G. de With and N. A. M. Sommerdijk, *J. Am. Chem. Soc.*, 2010, **132**, 11560–11565.
14 B. R. Heywood, S. Rajam and S. Mann, *J. Chem. Soc., Faraday Trans.*, 1991, **87**, 735–743.
15 J. H. Zhan, H. P. Lin and C. Y. Mou, *Adv. Mater.*, 2003, **15**, 621–623.
16 Y. W. Fan and R. Z. Wang, *Adv. Mater.*, 2005, **17**, 2384–2388.
17 G. Falini, *Int. J. Inorg. Mater.*, 2000, **2**, 455–461.
18 G. Falini, S. Albeck, S. Weiner and L. Addadi, *Science*, 1996, **271**, 67–69.
19 C. J. Stephens, Y.-Y. Kim, S. D. Evans, F. C. Meldrum and H. K. Christenson, *J. Am. Chem. Soc.*, 2011, **133**, 5210–5213.
20 C. J. Stephens, S. F. Ladden, F. C. Meldrum and H. K. Christenson, *Adv. Funct. Mater.*, 2010, **20**, 2108–2115.
21 C. C. Tester, R. E. Brock, C.-H. Wu, M. R. Krejci, S. Weigand and D. Joester, *CrystEngComm*, 2011, **13**, 3975–3978.
22 E. Loste and F. C. Meldrum, *Chem. Commun.*, 2001, 901–902.
23 E. Loste, R. J. Park, J. Warren and F. C. Meldrum, *Adv. Funct. Mater.*, 2004, **14**, 1211–1220.
24 Y.-Y. Kim, N. B. J. Hetherington, E. H. Noel, R. Kröger, J. M. Charnock, H. K. Christenson and F. C. Meldrum, *Angew. Chem., Int. Ed.*, 2011, **50**, 12572–12577.

25 J. Ihli, P. Bots, A. Kulak, L. G. Benning and F. C. Meldrum, *Adv. Funct. Mater.*, 2013, **23**, 1965–1973.
26 L. B. Gower, *Chem. Rev.*, 2008, **108**, 4551–4627.
27 X. R. Xu, J. T. Han and K. Cho, *Chem. Mater.*, 2004, **16**, 1740–1746.
28 Q. Hu, J. Zhang, H. Teng and U. Becker, *Am. Mineral.*, 2012, **97**, 1437–1445.
29 J. R. I. Lee, T. Y. J. Han, T. M. Willey, M. H. Nielsen, L. M. Klivansky, Y. Liu, S. Chung, L. J. Terminello, T. van Buuren and J. J. De Yoreo, *J. Phys. Chem. C*, 2013, **117**, 11076–11085.
30 D. Volkmer, M. Fricke, C. Agena and J. Mattay, *J. Mater. Chem.*, 2004, **14**, 2249–2259.
31 M. Maciejewski, H. R. Oswald and A. Reller, *Thermochim. Acta*, 1994, **234**, 315–328.